SPECIAL ISSUE

CSIRO PUBLISHING

*Marine and Freshwater Research*, 2019, **70**, 1708–1721
https://doi.org/10.1071/MF19067

# Otolith microchemistry: a useful tool for investigating stock structure of yellowfin tuna (*Thunnus albacares*) in the Indian Ocean

*Iraide Artetxe-Arrate*[A,E], *Igaratza Fraile*[A], *David A. Crook*[B], *Iker Zudaire*[A], *Haritz Arrizabalaga*[A], *Alan Greig*[C] *and Hilario Murua*[A,D]

[A]AZTI Tecnalia, Marine Research Division, Herrea Kaia, Portualdea s/n, E-20110 Pasaia, Gipuzkoa, Spain.
[B]Research Institute for the Environment and Livelihoods, Charles Darwin University, Darwin, NT 0909, Australia.
[C]School of Earth Sciences, The University of Melbourne, Vic. 3010, Australia.
[D]International Seafood Sustainability Foundation, 1440 G Street NW, Washington, DC 20005, USA.
[E]Corresponding author. Email: i.artetxe73@gmail.com

**Abstract.** A better understanding of the stock structure of yellowfin tuna (*Thunnus albacares*) in the Indian Ocean is needed to ensure the sustainable management of the fishery. In this study, carbon and oxygen stable isotopes ($\delta^{13}C$ and $\delta^{18}O$) and trace elements ($^{138}Ba$, $^{55}Mn$, $^{25}Mg$ and $^{88}Sr$) were measured in otoliths of young-of-the-year (YOY) and age-1 yellowfin tuna collected from the Mozambique Channel and north-west Indian Ocean regions. Elemental profiles showed variation in Ba, Mg and Mn in YOY otolith composition, but only Mn profiles differed between regions. Differences in YOY near-core chemistry were used for natal-origin investigation. Ba, Mg and Mn were sufficiently different to discriminate individuals from the two regions, in contrast with carbon and oxygen stable isotopes. A linear discriminant analysis resulted in 80% correct classification of yellowfin tuna to their natal origin. Classification success increased to 91% using a random forest algorithm. Finally, a unique larval source was detected among age-1 yellowfin tuna. The signal of these fish resembled that of YOY from a north-west Indian Ocean origin, highlighting the importance of local production. The present study supports the use of otolith chemistry as a promising approach to analyse yellowfin stock structure in the Indian Ocean.

Received 22 June 2018, accepted 7 October 2019, published online 12 November 2019

## Introduction

Stock identification is an essential component of modern fisheries management (Pita *et al.* 2016). Although several definitions of 'stock' have been used in the fisheries literature, the stock concept essentially describes demographically discrete units of fish assumed to be homogeneous for particular management purposes (Begg *et al.* 1999). A fundamental requirement for sustainable fisheries management is the match between management action units and biologically relevant processes (Reiss *et al.* 2009). Different stocks may possess specific genetic, physiological and behavioural traits that can influence life processes such as growth rates, fecundity, abundance and disease resistance (Stepien 1995), and thus different resilience to exploitation and environmental changes. As such, when stock structure is more complex than recognised, the sustainability of the resource and the profitability of the fishery can be jeopardised (Kerr *et al.* 2017; Taillebois *et al.* 2017).

Among the existing methods for fish stock structure assessment (e.g. genetic markers, tagging, life history parameters, parasites etc.), otolith microchemistry has been recognised as a useful stock discriminant (Kerr and Campana 2014; Tanner *et al.* 2016). These hard calcareous structures are found in the inner ear of vertebrates and are used for balance and hearing in teleost fish. Otoliths are acellular and metabolically inert (i.e. newly deposited material is neither reabsorbed nor reworked after deposition) and grow continually throughout the life of the fish (Campana and Neilson 1985). Ambient water chemistry and environmental conditions affect elemental incorporation into the otolith (Elsdon and Gillanders 2004; Walther and Thorrold 2006) and variations in the concentrations of selected elements and isotopes (also known as 'chemical fingerprints') can therefore be used as natural markers to discriminate among groups of fish for stock identification purposes (Kerr and Campana 2014). However, factors that affect the elemental incorporation into otoliths are not yet completely understood because various factors other than ambient water chemistry, including dietary sources, physiological processes and genetic variation, may also play important roles in elemental incorporation (Ranaldi and

Gagnon 2008; Clarke *et al.* 2011; Sturrock *et al.* 2015; Izzo *et al.* 2018).

The potential of otolith chemistry to improve our understanding of population structure (e.g. Wells *et al.* 2015), natal origin (e.g. Rooker *et al.* 2003; Shiao *et al.* 2010; Wells *et al.* 2012) and movement patterns (e.g. Arai *et al.* 2005; Macdonald *et al.* 2013; Fraile *et al.* 2016) of different tuna species has been demonstrated. However, few studies have used otolith microchemistry to assess the stock structure of yellowfin tuna (*Thunnus albacares* (Bonnaterre, 1788)), and these studies are limited to the Pacific (Wells *et al.* 2012; Rooker *et al.* 2016) and Atlantic (Shuford *et al.* 2007; Kitchens *et al.* 2018) oceans.

Yellowfin tuna is a highly migratory species that inhabits the epipelagic zone of tropical and subtropical marine waters around the world (Froese and Pauly 1999). It is a significant component of the global fishing industry and economy (Galland *et al.* 2016) and constitutes the second largest tuna fishery worldwide (Food and Agriculture Organization of the United Nations 2016). The high levels of exploitation of yellowfin tuna render the species vulnerable to unsustainable harvest. In the Indian Ocean, in particular, increased harvest in recent years has led to overexploitation of the stock (International Seafood Sustainability Foundation 2017). The most recent stock assessment model by the Indian Ocean Tuna Commission (IOTC), which takes into account both stock abundance and fishing mortality, confirmed that the yellowfin tuna stock in the IOTC area is overfished (Indian Ocean Tuna Commission 2017*a*).

The current stock assessment model for yellowfin tuna in the Indian Ocean assumes a single stock (Indian Ocean Tuna Commission 2017*a*). This assumption is based on tag recoveries from the Regional Tuna Tagging Program of the Indian Ocean (RTTP-IO), which showed large and rapid movements of the species around the Indian Ocean (Fonteneau and Hallier 2015). However, uncertainties remain regarding the stock structure of yellowfin tuna in this region, because tag–recapture studies may not reveal important aspects of the movement dynamics of wide-ranging species (see Rooker *et al.* 2008*a*). Indeed, genetic studies using mitochondrial (mt)DNA suggest that a more complex stock structure may exist within yellowfin tuna populations. For example, genetically discrete groups of this species have been reported in the north Indian Ocean (Dammannagoda *et al.* 2008) and within Indian Ocean waters (Kunal *et al.* 2013).

In the present study we analysed stable isotopes and trace elements in otoliths of young-of-the-year (YOY) and age-1 yellowfin tuna, which are both considered immature (Zudaire *et al.* 2013). During the YOY period, it is assumed that movements are restricted to a small area around the natal site, whereas for age-1 individuals large-scale movements can be expected (Fonteneau and Hallier 2015). Fish were collected in two regions of the western Indian Ocean, the north-west (NW) Indian Ocean and Mozambique Channel, because major yellowfin tuna spawning grounds have been identified westward of 75°E (Zudaire *et al.* 2013). In particular, the equatorial area (0–10°S) and the Mozambique Channel have been identified as primary and secondary spawning areas (Reglero *et al.* 2014; Indian Ocean Tuna Commission 2017*b*). The western region accounted for the 80% of the Indian Ocean catches in 2017 (Indian Ocean Tuna Commission 2018), being the most important area for the Indian Ocean yellowfin tuna fishery. The aim of the study was to assess the feasibility of otolith microchemistry as a potential tool for investigating yellowfin tuna stock structure in the Indian Ocean. Specifically, our objectives were to: (1) explore otolith chemistry profiles of YOY yellowfin tuna; (2) seek the best methodology for fish origin analyses and test region-specific differences on chemical composition of YOY yellowfin tuna otoliths; (3) evaluate the usefulness of different classification methods in assigning YOY yellowfin tuna origin to their respective collection regions; and (4) investigate potential natal-origin differences in age-1 yellowfin tuna.

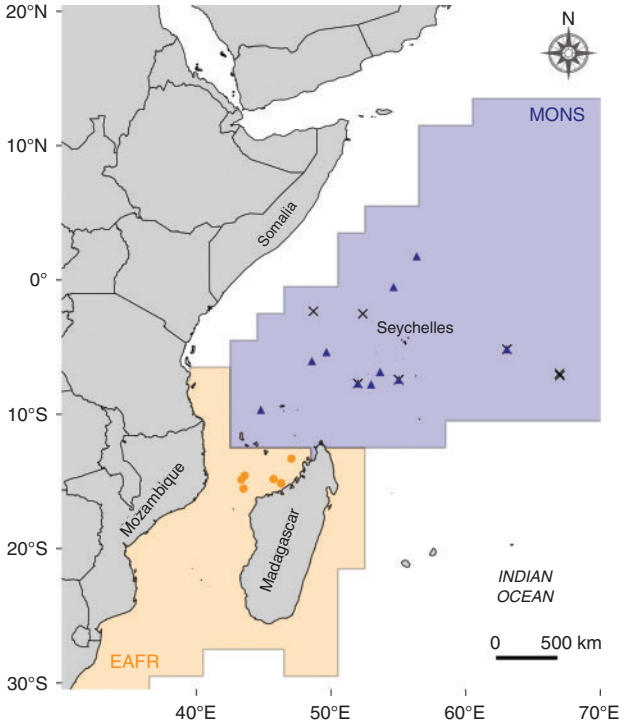


**Fig. 1.** Study area in the western Indian Ocean, where two Longhurst provinces, the Eastern Africa Coastal Province (EAFR) and the Indian Monsoon Gyres Province (MONS) are represented. Sampling locations of the different groups of yellowfin tuna (*Thunnus albacares*) used in this study are indicated as circles in the Mozambique Channel and triangles in the north-west Indian Ocean for young-of-the-year, and as crosses for age-1 fish of unknown origin.

## Material and methods

### *Study area*

Samples were collected across two regions of the western Indian Ocean: (1) offshore western Madagascar (15°53′S–13°30′S, 43°33′E–47°05′E), hereafter 'Mozambique Channel'; and (2) offshore Somalia and Seychelles regions (7°77′S–7°22′N, 48°57′E–58°37′E), hereafter 'NW Indian Ocean' (Fig. 1). These two regions belong to two distinct provinces according to the Longhurst (2007) biogeographical classification of the pelagic ecosystem: the Mozambique Channel belongs to the East African Coastal Province (EAFR) and the NW Indian Ocean is part of the Indian Monsoonal Gyre Province (MONS). These two regions are defined by different oceanographic characteristics that affect the biological production of the area (for further

**Table 1. Summary of young-of-the-year (YOY) and age-1 yellowfin tuna (*Thunnus albacares*) used for otolith chemistry analyses from two regions of the western Indian Ocean: the Mozambique Channel and the north-west (NW) Indian Ocean**

Size is fork length (FL). The cohort was calculated by back-calculation after age estimation following the growth curve described by Sardenne *et al.* (2015)

| Analytical method | Capture location | FL range (cm) | Age group | Collection dates | Cohort | Number of fish collected |
|---|---|---|---|---|---|---|
| Trace elements | Mozambique Channel | 31–39 | YOY | February–April 2010 | 2009 | 14 |
| | NW Indian Ocean | 29–35 | YOY | February 2009 | 2008 | 27 |
| | NW Indian Ocean | 52–64 | Age-1 | February–July 2009 | 2007 | 15 |
| Stable isotopes | Mozambique Channel | 31–40 | YOY | April–May 2010 | 2009 | 20 |
| | NW Indian Ocean | 29–39 | YOY | February–May 2009 | 2008 | 32 |

information, see Fig. S1–S5, available as Supplementary material to this paper). North of 10°S the Indian Ocean is characterised by two seasons with distinct wind regimes driving the ocean climate and circulation: the monsoon system (Schott and McCreary 2001). The south-west (summer) monsoon drives upwelling events that lead to high primary productivity off the coast of Somalia. By contrast, during the north-east (winter) monsoon, conditions are not favourable for upwelling and primary productivity is generally lower (Wiggert *et al.* 2006). The Mozambique Channel is characterised by the presence of anticyclonic eddies that generate an upward movement of nutrient-rich waters around their edge, and advection of nutrient-rich coastal waters when they run along the coast (Quartly and Srokosz 2004; Tew Kai and Marsac 2010).

### *Fish sampling*

Yellowfin tuna ($n = 106$) were collected in the western Indian Ocean by scientific observers on board Spanish commercial purse seiners between February 2009 and July 2010. Fish were measured (fork length (FL); to the nearest centimetre) and weighed (to the nearest 0.1 kg) on board. Sagittal otoliths were extracted, cleaned of adhering organic tissue, rinsed with ultrapure water and stored dry in plastic vials. The otolith collection available for this study comprised fish from different collection dates, age classes and cohorts. Following the growth curve described by Sardenne *et al.* (2015), fish were classified as YOY (<43 cm FL) or age-1 (43–75 cm FL). Birth year was then back-calculated from the catch date using the age–length relationship of Sardenne *et al.* (2015). In order to reduce potential variability due to temporal variation among samples, only fish born in the same monsoonal regime (i.e. summer monsoon) were selected for analysis. In addition, to minimise the possibility that YOY tuna had migrated outside their origin areas before sampling, only fish <40 cm were considered in the study. To date, no tagging experiments have considered fish of that size in movement range studies of yellowfin tuna (see Hallier and Fonteneau 2015). Nevertheless, our threshold size is even more conservative than those already considered in Atlantic Ocean yellowfin tuna stock structure analyses (Kitchens *et al.* 2018; Pecoraro *et al.* 2018). Thus, the final dataset consisted of 52 YOY and 15 age-1 fish (Table 1).

### *Otolith chemistry analysis*

Whole otoliths were briefly soaked in nitric acid (1%) and cleaned with ultrapure (Milli-Q) water to eliminate any remaining biological material (Rooker *et al.* 2001). Left and right otoliths were embedded in two-part resin (EpoFix; Struers, Ballerup, Denmark) and sectioned using a Buehler low-speed Isomet saw (Buehler, Lake Bluff, IL, USA) fitted with a diamond-edged blade to obtain a transverse section that included the core. When both otoliths from the same fish were available, one otolith was randomly selected for stable C and O isotope analysis and the other was used for trace element analysis. When only one otolith was available, stable isotope analyses were conducted.

Transverse sections were polished with a series of grinding and polishing films moistened with ultrapure water, and then with a microcloth and 0.3-mm alumina powder to ensure a smooth surface. Sections were glued in a sample plate using Crystalbond thermoplastic glue (Crystalbond 509; Buehler). For YOY, 41 otoliths were used for trace element chemistry and 52 for stable isotope analyses (Table 1). For age-1 fish, trace element composition of 15 yellowfin tuna was analysed (Table 1).

### *Trace element analysis*

Laser ablation–inductively coupled plasma–mass spectrometry (LA-ICP-MS) was used to determine the trace element chemistry of the otolith. Analyses were performed using a 7700X quadrupole inductively coupled plasma mass spectrometer (ICP-MS, Agilent Technologies, Santa Clara, CA, USA) coupled to a laser ablation system with a Laurin Technic 2 volume cell (RESOlution LA system, Resonetics, Nashua, NH, USA) available at the School of Earth Sciences, The University of Melbourne (Melbourne, Vic., Australia). The laser was operated using a spot size of 26 μm in diameter with laser energy at 2.4 J $cm^{-2}$ and a repetition rate of 10 Hz. Otoliths were placed in the sealed chamber and ablated continuously across the growth axis from the primordium to proximal edge at a scan speed of 6 μm $s^{-1}$ (Fig. 2*a*). Ablation occurred in an atmosphere of pure He to minimise condensation of ablated material. The ablated material was transported to the ICP-MS mixed with argon carrier gas. A preablation step was implemented to minimise potential surface contamination. National Institute of Standards and Technology (NIST) 612 glass standard with known chemical composition was used for calibration. Standards were analysed twice at the beginning and end of each session, and once after one-third and two-thirds of the duration of the run. In addition, measurement precision was determined based on the analyses of NIST610 and the calcium carbonate pressed pellet standard MACS-3 (US Geological Survey,

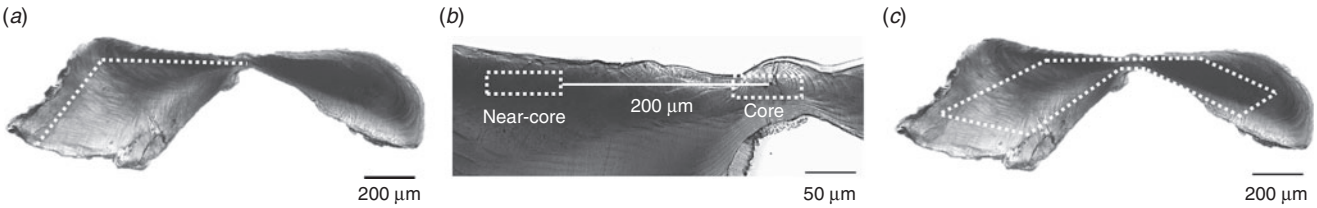


**Fig. 2.** Transverse section of a young-of-the-year yellowfin tuna (*Thunnus albacares*) sagittal otolith showing (*a*) the transect of the laser ablation spots performed along the growth axis, (*b*) the position of the data slices represented as the core and near-core and (*c*) pattern of the portion milled for stable isotope analysis.

Reston, VA, USA; Wolf and Wilson 2007; Limburg *et al.* 2011). The variation in ablation yields between standards and unknown samples was corrected with the use of calcium as an internal standard (Craig *et al.* 2000). Relative abundances of 10 isotopes ($^{7}$Li, $^{25}$Mg, $^{55}$Mn, $^{57}$Fe, $^{59}$Co, $^{60}$Ni, $^{63}$Cu, $^{66}$Zn, $^{88}$Sr and $^{138}$Ba) were measured along the whole transect using the LA-ICP-MS system, and elemental concentrations (ppm) were then calculated. Data reduction and processing were performed with the software package Iolite (ver. 2.2, School of Earth Sciences, The University of Melbourne), which operates within IGOR Pro (ver. 6.2, WaveMetrics, Lake Oswego, OR, USA; Paton *et al.* 2011; Paul *et al.* 2012). The limit of detection (LOD) was calculated based on the ablation yield equivalent to three times the standard deviation of the blank signal. Averaged LOD values (ppm) of each element across all samples were as follows: Li, 0.049; Mg, 0.423; Mn, 0.079; Fe 0.920; Co, 0.020; Ni, 0.030; Cu, 0.023; Zn, 0.120; Sr, 0.0145; and Ba, 0.004. Five elements (Ba, Mg, Mn, Fe and Sr) were consistently present at concentrations above LODs within the whole transects. However, low measurement precision and accuracy was reported for Fe in MACS-3 and NIST610 (Table S1, available as Supplementary material to this paper), due to time-dependant increases in apparent concentrations. This is likely due to decreasing oxide–hydroxide interferences (e.g. $^{40}$Ca-$^{16}$O-H) with time affecting the low Fe/Ca NIST612 calibration standard proportionally more than the higher Fe/Ca NIST610 and MACS-3 standards. Thus, Fe was discarded for analyses. In addition, an ablation transect was performed on a test sample composed only of resin and thermoplastic glue. This analysis showed that resin was enriched in Zn, whereas high levels of Cu were found on the thermoplastic glue. Therefore, unusually high concentrations of Cu and Zn throughout the transect were used as indicators of potential sample contamination. Aragonitic calcium carbonate stoichiometry (400 000 mg Ca $g^{-1}$ otolith) was used for calcium concentration calculation, and hereafter the concentrations of the rest of the elements are expressed as element : Ca ratios (Ludsin *et al.* 2006).

In addition to whole transects, two data slices 78 µm in length were isolated from the primordium (hereafter 'core') and 200 µm beyond the primordium (hereafter 'near-core'), by averaging all trace element concentration estimates across each data slice (Fig. 2*b*). Daily increment formations were counted along the first 550 µm of the transect in a subset of YOY otoliths ($n = 8$) under a light microscope (Fig. S6, available as Supplementary material to this paper). It was determined that the two 78-µm slices represent the otolith material accreted during the first ~10 days and first ~2–3 weeks after hatching respectively, when the fish are still in the larval phase (Kaji *et al.* 1999).

### *Stable isotope analysis*

Microsampling of otolith powder for carbon ($\delta^{13}$C) and oxygen ($\delta^{18}$O) stable isotope analysis was performed using a high-resolution computerised micromill (New Wave MicroMill System, New Wave Research G. C. Co., Ltd, Cambs, UK) only in YOY yellowfin tuna. The portion of the smallest fish (29 cm FL) in our sample was used to create a standard template that was then used with the remaining otoliths (Fig. 2*c*) to ensure that the same portion of the otolith was analysed in each individual. This is approximately related to the first 5–6 months of life according to the age–length relationship described by Sardenne *et al.* (2015).

Fourteen drill passes were run at a depth of 50 µm per pass over a preprogrammed drill path using a 200-µm diameter carbide bit (Komet dental; Gebr. Basseler, Lemgo, Germany). Powdered material was then analysed for $\delta^{13}$C and $\delta^{18}$O on an automated carbonate preparation device (KIEL-III, ThermoFisher Scientific, Waltham, MA, USA) coupled to a gas-ratio mass spectrometer (Finnigan MAT 252, ThermoFisher Scientific) at the Environmental Isotope Laboratory of the University of Arizona. All isotope values were reported according to standards of the International Atomic Energy Agency in Vienna (see https://www-pub.iaea.org/MTCD/publications/PDF/te_825_prn.pdf, accessed May 2012). Values of $\delta^{13}$C and $\delta^{18}$O represent ratios of $^{13}$C/$^{12}$C and $^{18}$O/$^{16}$O in the sample relative to the Vienna Pee Dee Belemnite (VPDB) scale.

### *Statistical analysis*

All statistical analyses were performed using open access R software (R Foundation for Statistical Computing, Vienna, Austria, see http://www.R-project.org/, accessed September 2014). Prior to all multivariate analyses, trace element data were scaled to give the same weight to all elements. An $\alpha$ level of 0.05 was used for all two-tailed statistical tests.

### *Elemental profile analysis*

Whole transects of YOY yellowfin tuna were transformed into equally spaced observations, generating a regular time series of elemental concentration from 0 to ~550 µm (i.e. approximately the first month after hatch). Data transformation and ordination were performed using *zoo* (ver. 1.8-6, see http://zoo.R-Forge.R-project.org/, accessed 6 November 2019; Zeileis and Grothendieck 2005) and *vegan* (J. Oksanen, F. Blanchet, M. Friendly, R. Kindt, P. Legendre, D. McGlinn, P. R. Minchin, R. B. O'Hara, G. L. Simpson, P. Solymos, M. Henry, H. Stevens, E. Szoecs, and H. Wagner, see https://cran.r-project.org/package=vegan, accessed 13 March 2018) packages. To examine

leading patterns and temporal variations for the elements, regular time series data were simplified by averaging concentrations every 25 µm. Estimates of the s.d. were also calculated. Mean estimates of concentrations and profiles of element : Ca ratios were obtained for each region. In addition, a principal component analysis (PCA) was applied to each element in the time series data. To determine whether differences existed between regions, a permutational multivariate analysis of variance (PERMANOVA) test was performed on the scores of the first two axes.

### *Natal-origin microchemistry of YOY*

YOY yellowfin tuna were used to determine whether the fish collected in Mozambique Channel and NW Indian Ocean origin could be differentiated based on otolith stable isotope and trace element concentrations measured in the otolith core and near-core. Normality and homoscedasticity were tested using Shapiro–Wilks and Fligner–Killeen tests respectively. Stable isotope data did meet these assumptions, so Student's *t*-test was used for inter-region comparisons. Trace element data violated parametric assumptions; consequently, a robust statistical method was used to investigate these data, specifically a bootstrapped Yuen *t*-test (trimmed level for the mean = 0.2, number of bootstrap samples = 599). Robust statistics are not unduly affected by outliers and violations of parametric assumptions, reducing the probability of making a Type I error and improving test power when data are not normal or homogeneous (Daszykowski *et al.* 2007; Erceg-Hurn and Mirosevich 2008; Wilcox 2012). Accordingly, a Hotelling $T^2$ test was used to test the significance of differences in $\delta^{13}C$ and $\delta^{18}O$ values among regions and PERMANOVA was used to test the significance of differences in element : Ca ratios. Finally, core and near-core trace element data were examined using non-metric multidimensional scaling (nMDS) to obtain a reduced two-dimension graphical representation of the relationships between samples (Hout *et al.* 2013). The dissimilarity matrix construction was based on Euclidean distances. The otolith portion showing greatest variation among regions was used as the origin indicator in subsequent analyses.

### *Comparison of classification methods*

Discrimination capacity between fish collected in the two regions was assessed using YOY otolith near-core microchemistry data using different classification methods. Four different methodologies were used, two classical methods (linear discriminant analysis (LDA) and quadratic discriminant analysis (QDA)) and two data-mining methods (random forest (RF) and artificial neural network (ANN)). LDA and QDA were completed using *lda* and *qda* functions from the MASS library; RF was implemented using the *randomForest* function from the *randomForest* library, using default settings (Liaw and Wiener 2002) and ANN was performed using the *nnet* function from the *nnet* library, using default settings and 30 hidden neurons at the intermediate layer (Venables and Ripley 2002). Detailed descriptions of each technique and their assumptions can be found in Jones *et al.* (2017) and Mercier *et al.* (2011). In all cases, data were randomly split into a training dataset (75%) and a testing dataset (25%) to perform a cross-validation procedure and measure prediction quality. To avoid sampling effects, the training subset was resampled 10 times and mean prediction accuracy (i.e. percentage of correct assignment of the fish to their known region) was obtained. In addition, the kappa index was calculated as a measure of classification success. Kappa values are always $\leq 1$, with a value of 1 implying perfect agreement. The kappa index is unbiased when the number of samples differs between groups, and can present more reliable results because it considers the possibility of the agreement occurring by chance (Fielding and Bell 1997; Jones *et al.* 2017). Following Mercier *et al.* (2011), the elemental combination maximising habitat discrimination was selected by performing a stepwise forward variable selection procedure using the Wilk's lambda criterion for LDA and QDA. In the case of RF, the best elemental combination was obtained by stepwise procedure using the Gini index (Cutler *et al.* 2007), and in the case of ANN following Olden *et al.* (2004).

### *Natal sources of age-1 fish*

RF clustering analysis of the near-core trace element data was performed in age-1 fish to determine the number of larval sources contributing to the sample. This approach proved to be useful for natal origin-related investigations when there is no previous baseline of potential larval sources (Gibb *et al.* 2017; Régnier *et al.* 2017; Wright *et al.* 2018). Moreover, the RF clustering approach does not require continuous multivariate data with normal distribution (Shi and Horvath 2006), an assumption that is often violated when working with otolith microchemistry data. The RF classification process was applied following Shi and Horvath (2006). First, a synthetic dataset was created by random sampling from the product of empirical marginal distributions of the elements. Then, unsupervised RF was used to separate the synthetic data (used as a class factor) from the observed data, and a dissimilarity matrix was created. Second, the dissimilarity matrix was used as input for partitioning around the medoid (PAM) clustering. Finally, the appropriate number of clusters was determined using the gap statistic (Tibshirani *et al.* 2001), with the *fviz_nbclust* function from the *factoextra* library (bootstrap number = 100). Canonical variable coefficients of YOY and age-1 yellowfin tuna trace element composition were plotted to visualise relationships (Hamer *et al.* 2005).

## Results

### *Elemental profile analysis*

Patterns of element : Ca variation in YOY along the analysed transect were very similar between the two regions, except for Mn : Ca (Fig. 3, 4). Ba : Ca concentrations declined with increasing time after hatch, with YOY from the NW Indian Ocean having higher mean Ba values than those from the Mozambique Channel along most of the transect. As of the third week after hatch, the decreasing trend smoothed and became more similar between regions (Fig. 3*a*). Mg : Ca concentrations of both regions declined almost linearly within the first month of life. However, YOY from the Mozambique Channel had higher mean concentrations than those from the NW Indian Ocean along the whole transect (Fig. 3*b*). Mean Mn : Ca concentrations showed different trends between regions. For the Mozambique Channel, they were fairly constant during the first month after

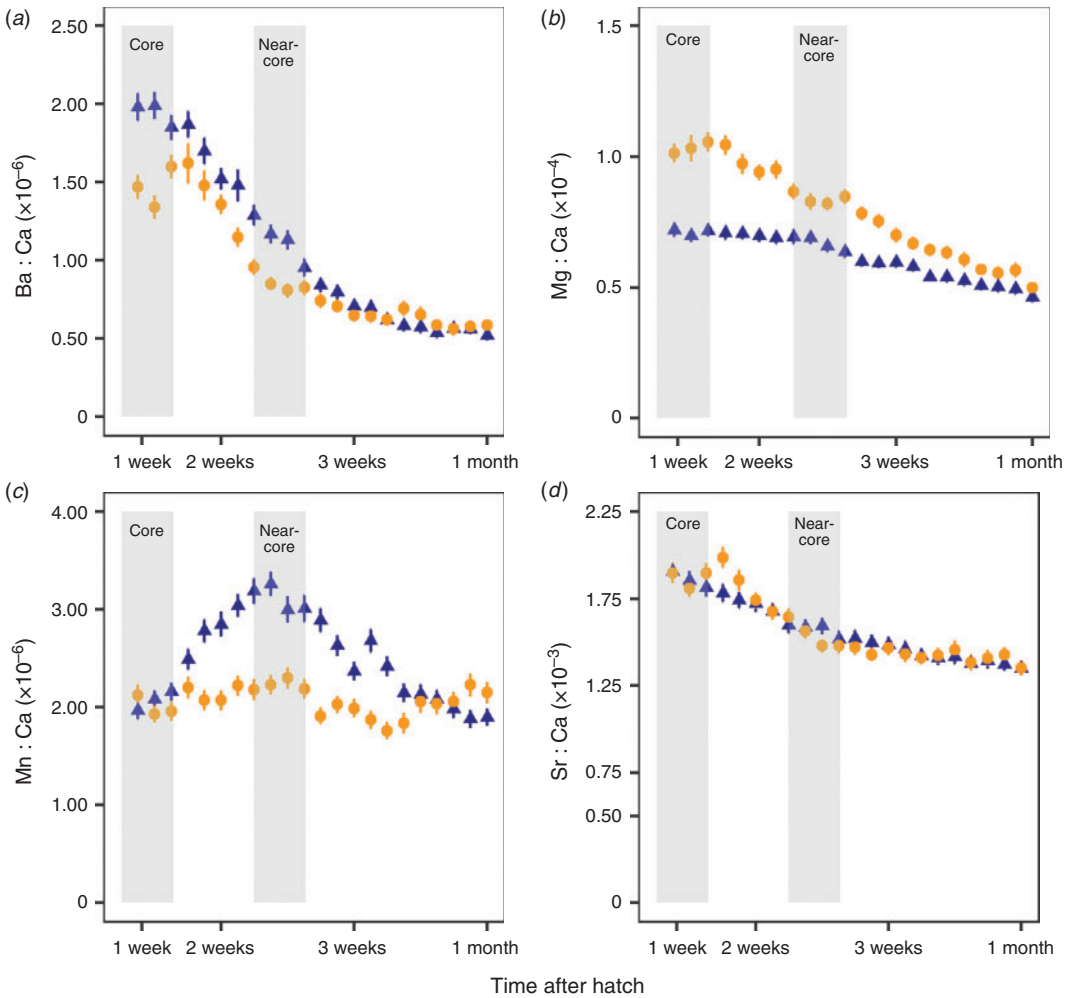


**Fig. 3.** Mean (±s.d.) element : Ca concentrations across the first month of life of young-of-the-year yellowfin tuna (*Thunnus albacares*) collected in the Mozambique Channel (circles) and north-west Indian Ocean (triangles). Shaded areas represent the signatures that will correspond to the core and near-core portions of the otolith.

hatch. However, for NW Indian Ocean YOY, Mn : Ca increased sharply in the first ~2.5 weeks after hatch, with a progressive decrease thereafter (Fig. 3*c*). Sr : Ca showed little variation both among regions and along the transect, although slightly decreasing trends of concentrations were observed (Fig. 3*d*).

The PCA showed that all element : Ca time series were related among regions with the exception of Mn : Ca (Fig. 4). For this element, the scores of the first two axes of the PCA varied significantly between fish from the two regions (PERMANOVA, $F_{1,39} = 14.96$, $P = 0.01$). The first two axes explained 39% of the total variation.

### *Natal-origin microchemistry of YOY*

Significant differences in multi-elemental trace signatures (i.e. Ba : Ca, Mg : Ca, Mn : Ca and Sr : Ca) were found between the Mozambique Channel and NW Indian Ocean in the near-core portion of the otolith (PERMANOVA, $F_{1,39} = 4.09$, $P = 0.010$) but not in the core (PERMANOVA, $F_{1,39} = 2.32$, $P = 0.050$). Similarly, differences in trace element composition were more marked in the two-dimension nMDS plot of the otolith near-core than in the core (Fig. 5). Indeed, only Mg : Ca ratios were significantly different in the otolith core (Yuen test, $t = 2.22$, d.f. = 11.36, $P = 0.046$), with YOY from the Mozambique Channel having higher values than those from the NW Indian Ocean (Fig. 6*b*). YOY from the Mozambique Channel also had higher Mg concentrations than those from the NW Indian Ocean in the near-core portion (Fig. 6*b*; Yuen test, $t = 4.05$, d.f. = 12.06, $P = 0.001$). Ba and Mn also varied significantly in the otolith near-core among regions (Yuen test, $t = 2.11$ (d.f. = 24.89; $P = 0.045$) and $t = 2.36$ (d.f. = 16.60; $P = 0.030$) respectively), but in this case YOY from the NW Indian Ocean had higher values of both elements (Fig. 6*a*, *c*). There were no significant variations in Sr concentrations between regions in near-core signatures (Fig. 6*d*; $t = 1.18$, d.f. = 16.08, $P = 0.256$).

Stable isotope composition of YOY yellowfin tuna did not vary between fish collected in the Mozambique Channel and NW Indian Ocean (Fig. 7; Hotelling $T^2$ test, $T_{2,41} = 0.76$, $P = 0.474$). Mean (±s.d.) otolith $\delta^{13}C$ values were $-10.27 \pm 0.43$ and $-10.13 \pm 0.35$‰ for YOY from the Mozambique Channel and

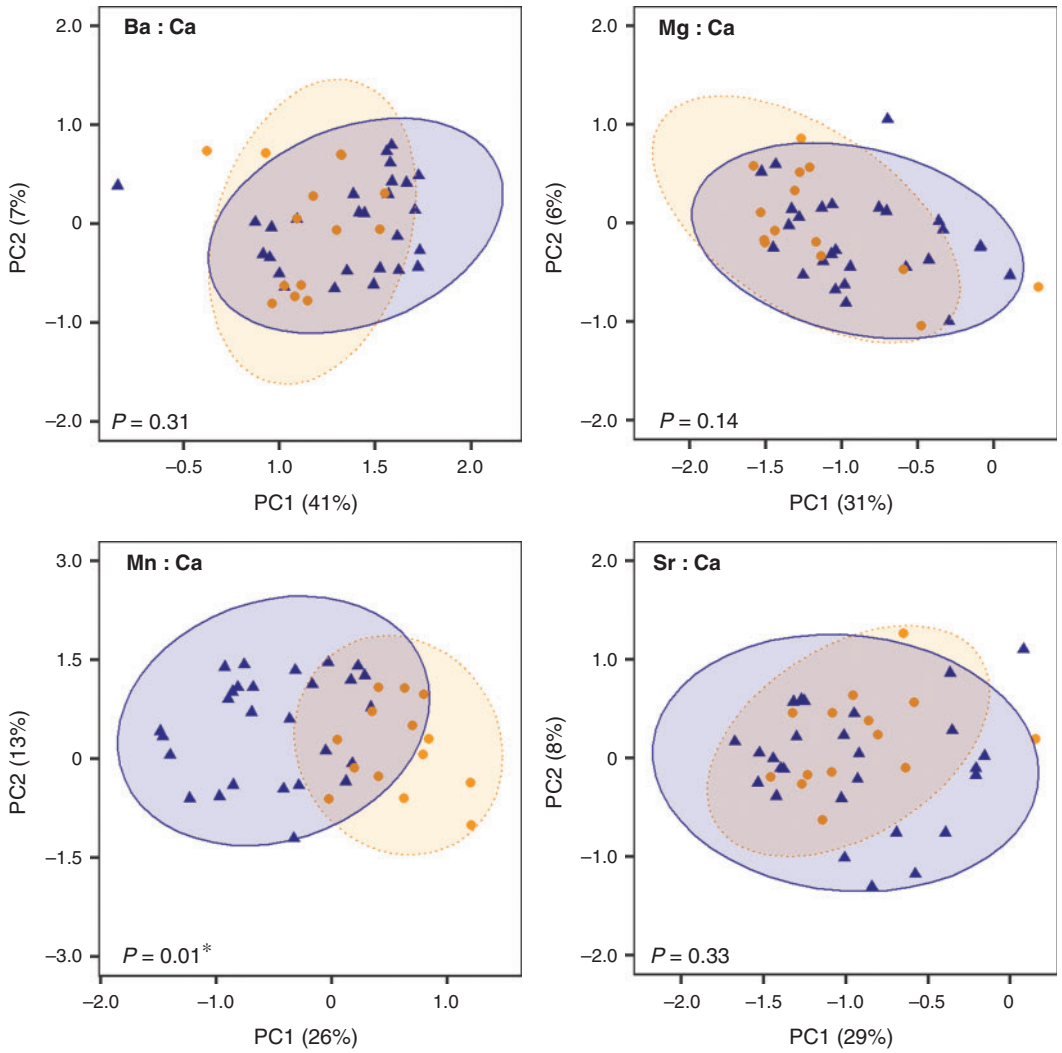


**Fig. 4.** Principal component (PC) analysis correlation biplot on element : Ca time series data of the first month of life in young-of-the-year yellowfin tuna (*Thunnus albacares*) collected in the Mozambique Channel (circles) and north-west Indian Ocean (triangles). Ellipses represent the 95% confidence intervals for each region (dotted ellipse, Mozambique Channel; solid ellipse, north-west Indian Ocean). *P*-values are for differences in PC1 and PC2 scores according to permutational multivariate analysis of variance (PERMANOVA).

NW Indian Ocean respectively (Student's *t*-test, $t_{26,84} = -1.15$, $P = 0.259$). The mean otolith $\delta^{18}O$ value for fish collected in the Mozambique Channel was $-2.32 \pm 0.14$‰, whereas for fish collected in the NW Indian Ocean it was $-2.29 \pm 0.23$‰ (Student's *t*-test, $t_{41,72} = -0.53$, $P = 0.600$).

### *Comparison of classification methods*

Cross-validated classification success based on YOY yellowfin tuna near-core trace element data ranged from 80 to 91% depending on the statistical method selected. However, results were more conservative according to the kappa index ($\kappa = 0.53$–0.72). LDA had the lowest differentiation capacity (Table 2). QDA and ANN showed similar results, with ANN presenting slightly higher accuracy and kappa value than QDA (Table 2). RF outperformed the other methods and produced the highest classification success (91%; $\kappa = 0.72$). Regardless of the method used for prediction, the best elemental combination always included Mg : Ca and Mn : Ca.

### *Natal sources of age-1 fish*

RF clustering of age-1 fish from unknown origin suggested a common larval source among the analysed samples. The canonical variable plot displaying spatial differences of the multi-elemental data showed that age-1 yellowfin near-core elemental composition was more similar to YOY of the NW Indian Ocean than to YOY of the Mozambique Channel, although there was considerable overlap among the regions (Fig. 8).

## Discussion

Improving understanding of the stock structure of exploited species is essential for defining appropriate management units and optimising the use of fishery resources. In this context, this

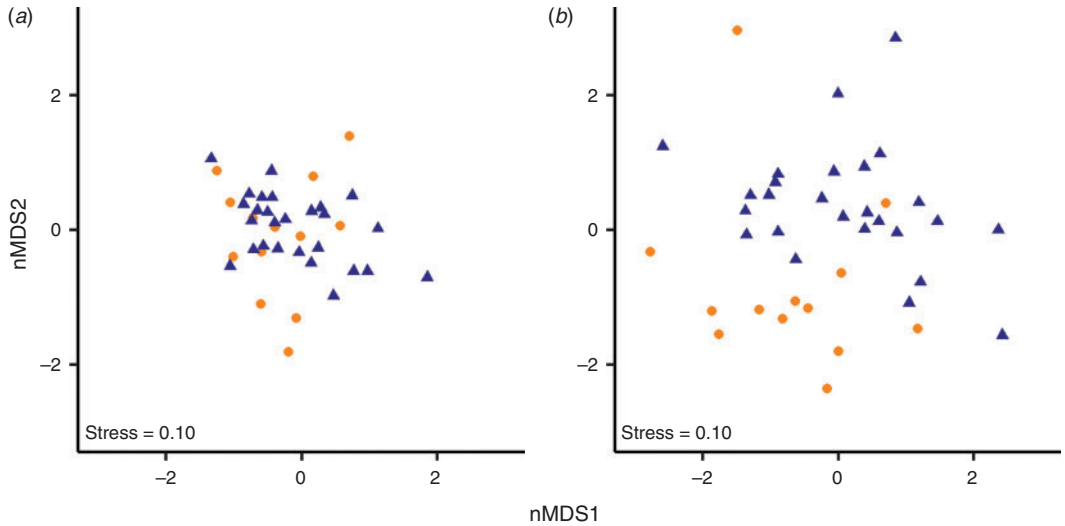


**Fig. 5.** Non-metric multidimensional scaling (nMDS) of young-of-the-year yellowfin tuna (*Thunnus albacares*) otolith (*a*) core and (*b*) near-core trace elements (Ba : Ca, Mg : Ca, Mn : Ca and Sr : Ca). Each point represents an individual fish belonging to the Mozambique Channel (circles) and north-west Indian Ocean (triangles) regions.

study used, for the first time, an otolith microchemistry approach for yellowfin tuna in the Indian Ocean and revealed the potential of this technique to provide valuable information about its stock structure. The main limitation of the study was that the YOY yellowfin tuna collected in the two regions were sampled from different cohorts. Therefore, observed differences between regions could result from the interannual variability in the oceanic system rather than variability among regions. However, this hypothesis seems unlikely, because interannual variability in environmental conditions was negligible for the observed periods (Table S2, available as Supplementary material to this paper).

### *Elemental profile analysis*

Almost all elements followed a similar pattern of variation within the first month after hatch in both regions. Element profile analyses of natural otolith tags can be used for environmental and life history reconstructions (Elsdon *et al.* 2008). For example, Ba and Sr incorporation into otoliths has been shown to be correlated with ambient concentrations (Webb *et al.* 2012; Izzo *et al.* 2018). These alkaline metals are incorporated into the mineral component of the otolith (Izzo *et al.* 2016; Loewen *et al.* 2016), and thus appear to be reliable 'geographical markers' (Thomas *et al.* 2017). Although both elements have been related to salinity (e.g. Elsdon and Gillanders 2005; Macdonald and Crook 2010), the fact that Ba : Ca varied along the transect whereas Sr : Ca did not may suggest that observed Ba variation did not reflect changes in salinity. Indeed, no noticeable seasonal variation of sea surface salinity was detected in the western Indian Ocean (Fig. S1). Elevated Ba : Ca concentrations in the primordium relative to adjacent parts of the otolith have been previously described in the literature (Ruttenberg *et al.* 2005). However, this does not exclude other external influences of Ba incorporation. For example, because dissolved Ba in seawater possesses a nutrient-like profile (i.e. very low concentration in surface waters and increased values with deeper water), an increase in the Ba : Ca concentration may reflect periods of residence near upwelling zones (Patterson *et al.* 2004; Kingsford *et al.* 2009; Wang *et al.* 2009). During the summer monsoon (the period when YOY were born), elevated phytoplankton blooms have been described to extend off the Somali coast (Fig. S2; Wiggert *et al.* 2006), which could also be the reason for increased Ba concentration. Equally, classic eddy upwelling occurs throughout the Mozambique Channel, enhancing chlorophyll-*a* concentrations in the centre of the cyclones (Lamont *et al.* 2014). Magnesium concentrations decreased linearly with time after hatch. This pattern matches with previously described Mg : Ca profiles in the literature, with higher levels at early life (near otolith primordium) followed by a transition to lower Mg levels (Limburg *et al.* 2018). The uptake rate of Mg into otoliths has been related to somatic growth and otolith precipitation (Bath Martin and Thorrold 2005; Limburg and Casini 2018). The incorporation of this element into otoliths seems to be strongly regulated by physiological processes between the otolith and water (Hamer and Jenkins 2007). Therefore, the concentration of Mg in fish otoliths has been questioned as a reliable environmental indicator (Woodcock *et al.* 2012; Thomas *et al.* 2017). Mn : Ca profiles proved to be significantly different between the NW Indian Ocean and Mozambique Channel YOY yellowfin tuna. Manganese is a transition metal and, as such, its incorporation into the otolith can be physiologically regulated, which may caution against its use as an environmental marker (Thomas *et al.* 2017). Manganese concentrations have also been found to be high near the otolith primordium, possibly due to maternal transfer (Ruttenberg *et al.* 2005). However, no higher Mn concentrations in the first weeks of life were observed for YOY from the Mozambique Channel relative to the rest of the transect. Although sensitive to growth effects, environmental influences seem also to affect otolith Mn concentrations (Limburg and Casini 2018). In particular, otolith Mn : Ca concentrations have been shown to be a reliable proxy for fish exposure to hypoxia (Limburg *et al.* 2011, 2015). During the summer monsoon,

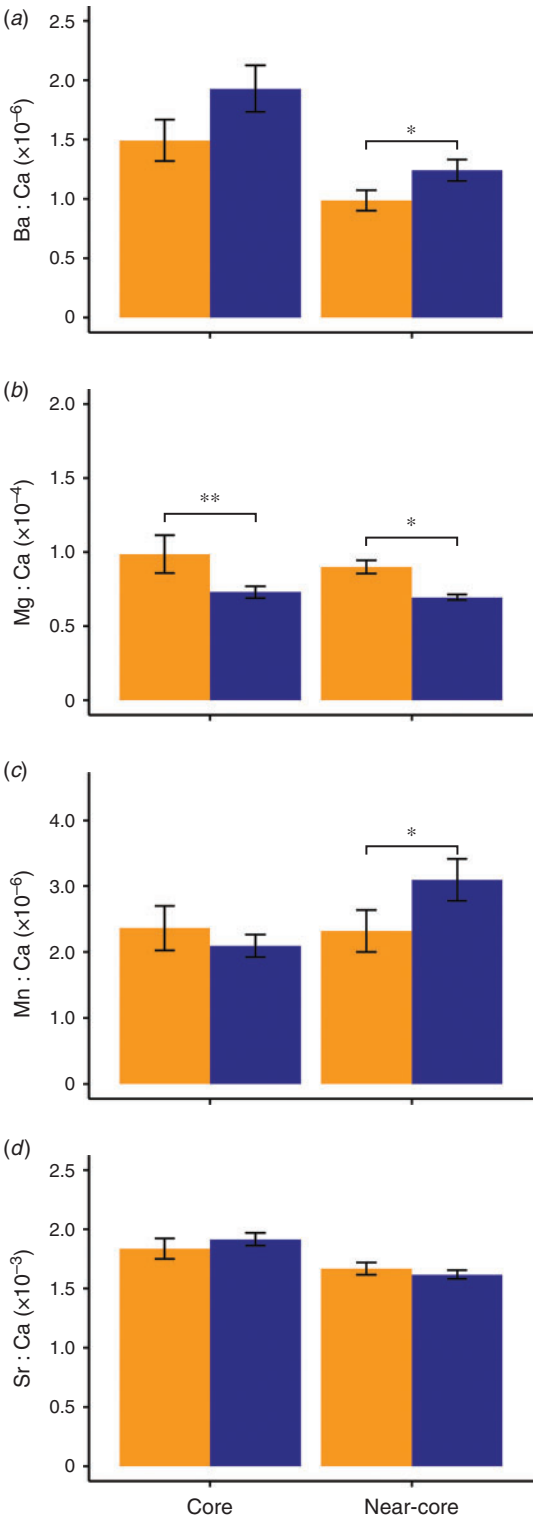


**Fig. 6.** Mean (±s.d.) element : Ca ratios in otolith cores and near-cores of young-of-the-year yellowfin tuna (*Thunnus albacares*) collected at two different regions, Mozambique Channel (left bars) and NW Indian Ocean (right bars). Asterisks indicate the significance of differences among regions according to bootstrapped Yuen *t*-tests (*, $P < 0.05$; **, $P < 0.01$).

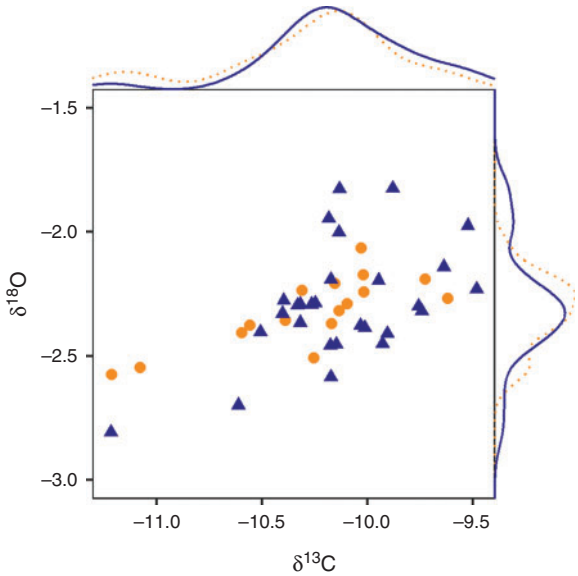


**Fig. 7.** Scatter plot of otolith $\delta^{13}C$ and $\delta^{18}O$ of young-of-the-year yellowfin tuna (*Thunnus albacares*) captured in the Mozambique Channel (circles) and north-west Indian Ocean (triangles) regions. Marginal distribution curves of $\delta^{13}C$ and $\delta^{18}O$ are also presented for the Mozambique Channel (dotted lines) and north-west Indian Ocean (solid lines).

**Table 2. Comparison of classification methods for assigning young-of-the-year (YOY) yellowfin tuna (*Thunnus albacares*) collected in the Mozambique Channel and north-west (NW) Indian Ocean to their origin location based on near-core otolith microchemistry**

Best elemental combination and performance, as a measure of maximal accuracy and the kappa index, are shown for each method. LDA, linear discriminant analysis; QDA, quadratic discriminant analysis; ANN, artificial neural network; RF, random forest

| Classification method | Element combination | Maximal accuracy (%) | Kappa index |
|---|---|---|---|
| LDA | Mg, Mn | 80 | 0.53 |
| QDA | Mg, Mn | 81 | 0.60 |
| RF | Ba, Mg, Mn, Sr | 91 | 0.72 |
| ANN | Ba, Mg, Mn, Sr | 83 | 0.63 |

dissolved oxygen concentration is lower in the NW Indian Ocean than Mozambique Channel (Fig. S3). Thermal vents, sediments, rivers and atmospheric dust are also known sources of manganese in seawater (van Hulten *et al.* 2017). The influence of aeolian deposition of Mn is greater in the NW Indian Ocean because of its proximity to the arid Arabian subcontinent (van Hulten *et al.* 2017). Therefore, changes in wind patterns may be another plausible cause of observed differences in Mn : Ca profiles of the two regions. Life history otolith chemistry profiles would be valuable for resolving stock structure of the species (e.g. Fowler *et al.* 2017), but there is still a considerable need for further empirical studies regarding elemental incorporation processes into otoliths for a comprehensive interpretation of the results.

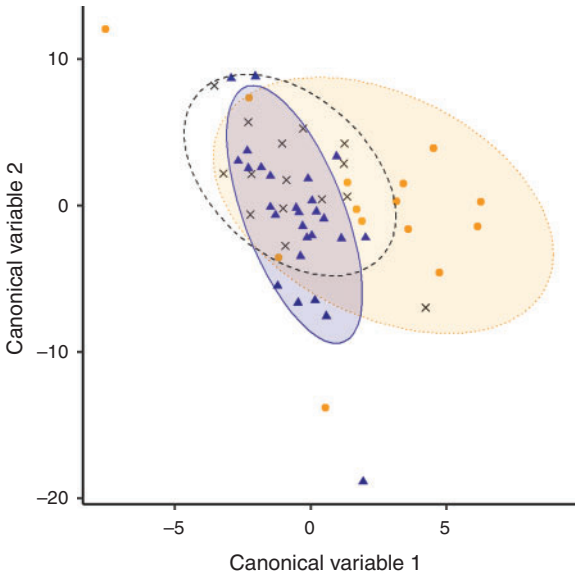


**Fig. 8.** Canonical variable plots comparing trace element tags (Ba : Ca, Mg : Ca, Mn : Ca and Sr : Ca) of age-1 yellowfin tuna (*Thunnus albacares*) from unknown origin (crosses) with those of young-of-the-year (YOY) yellowfin tuna captured in the Mozambique Channel (circles) and north-west Indian Ocean (triangles) regions. Confidence ellipses cover the 95% of each group (dashed ellipse, age-1 tuna; dotted ellipse, Mozambique Channel YOY; solid ellipse, north-west Indian Ocean YOY).

### *Natal-origin microchemistry of YOY*

The otolith near-core portion showed greater variability in trace elements among the two regions than did the core. Higher levels of Zn and Cu were found in core portions compared with the near-core (Fig. S7, available as Supplementary material to this paper). It is possible that some thermoplastic glue or resin residues had entered the pits and crevices occasioned in the primordium of some samples due to polishing (Di Franco *et al.* 2014). It is also possible that the chemical signature of this zone, which is formed during egg development, could have been affected by maternal inheritance (e.g. Campbell *et al.* 2002; Ruttenberg *et al.* 2005; Thorrold *et al.* 2006). Therefore, this signature can be affected by the environment that is experienced by the maturing female (Volk *et al.* 2000), hindering its use as an indicator of fish origin. Given these circumstances, trace element signatures from the primordium may not be appropriate for determining YOY yellowfin tuna origin, and the use of otolith material from a few weeks after hatch could represent a better alternative for early life history comparisons (see also Macdonald *et al.* 2008).

Region-specific chemical signatures were detected in the otolith near-core composition, with three elements (Ba, Mg and Mn) showing regional differences in otolith near-core chemistry of YOY yellowfin tuna. As stated above, in the NW Indian Ocean, upwelling events occurring during the south-west (summer) monsoon generate an upward movement of nutrient-rich waters from below the thermocline to shallower depths, which possibly implies the observed higher Ba : Ca concentrations in otolith near-core compared with YOY from the Mozambique Channel. YOY from the NW Indian Ocean also had higher concentrations of Mn : Ca in the otolith near-core than YOY from the Mozambique Channel, possibly due to their proximity to an arid region or an oxygen minimum zone (McCreary *et al.* 2013). Differences in Mg : Ca ratios in otoliths of fish from the Mozambique Channel and NW Indian Ocean may also reflect physiological differences rather than environmental differences (Woodcock *et al.* 2012). Nonetheless, each of the above elements differed significantly between groups, and they may be useful as tracers of nursery origin regardless of the cause of variation between regions.

Owing to the lack of difference in otolith isotope composition between the two regions in the first 5–6 months of life, $\delta^{13}C$ and $\delta^{18}O$ seem to be of negligible value for investigation of YOY yellowfin tuna origin in the western Indian Ocean. This is likely explained by the lack of variation in oxygen isotopic composition in the seawater of this region (LeGrande and Schmidt 2006).

### *Comparison of classification methods*

In this study, RF was the best method to predict natal origin, with highest accuracy and kappa index. When using otolith microchemistry for identification of fish origin, the choice of the optimal classification method is important in order to avoid misinterpreting the results. Traditional approaches (LDA and QDA) have been commonly used as classification tools in other tuna otolith chemistry studies (e.g. Rooker *et al.* 2008*b*, 2016; Wells *et al.* 2012; Macdonald *et al.* 2013). However, in recent years, machine learning techniques have emerged as promising classification tools in otolith-related studies (Zhang *et al.* 2016; Tournois *et al.* 2017; Bouchoucha *et al.* 2018). The accuracy of each technique will depend on the nature of the data analysed, and the results of this study agree with those of recent studies encouraging the use of machine learning methods when otolith chemical data are not multivariate normal or exhibit skewed distributions (Mercier *et al.* 2011; Jones *et al.* 2017). The reasonably easy use of RF, together with a lack of distributional assumption requirements and the robustness of RF against overfitting (Breiman 2001), make this technique a useful approach for population structure analyses of yellowfin tuna in the Indian Ocean.

### *Natal sources of age-1 fish*

Given the high migratory behaviour and dispersal capacity of yellowfin tuna (Fonteneau and Hallier 2015), obtaining a sufficiently representative baseline at such a large scale would have been logistically unfeasible in the present study. Alternatively, using unsupervised learning methods to cluster larval elemental signatures is well suited for studies where no representative baseline samples are available (Gibb *et al.* 2017). In the present study, the RF clustering approach used on the near-core otolith portion inferred the presence of a cluster for age-1 yellowfin tuna of unknown origin. This implies either that the samples share a common origin, with a common larval source contributing to the samples, or a lack of difference in elemental composition between different source locations. Although the approach does not directly provide information on the location of this potential common larval source, a canonical covariates plot revealed higher similarity with NW Indian Ocean YOY signatures than with Mozambique Channel YOY. The sizes of

the age-1 individuals in this study (i.e. 52–64 cm FL) were of a similar range as those from the RTTP-IO (i.e. 56–75 cm FL), which reported large movements and a low average rate of homing fidelity in yellowfin tuna of the Indian Ocean (Fonteneau and Hallier 2015). Therefore, the presence of different larval sources would have not been surprising in the age-1 sample composition. However, it has also been shown that distances travelled by yellowfin tuna captured around Seychelles Islands (NW Indian Ocean) were lower than for tuna from other areas (Hallier and Million 2012). This could possibly explain the origin and retention of age-1 samples in the region. This would highlight the importance of local production of yellowfin tuna recruits in the NW Indian Ocean fishery. A high degree of local production and retention of yellowfin tuna has also been reported in other oceans (Rooker *et al.* 2016; Wells *et al.* 2012).

## Conclusions

This study supports the utility of otolith chemical analyses to provide valuable information about the stock structure of yellowfin tuna in the western Indian Ocean and suggests a more complex stock structure in the area than previously assumed. However, future work should delve into analysis at a whole-ocean scale, preferably sampling distinct regions at the same period. Moreover, further development and application of this approach is now needed, in particular by quantifying spatial and temporal variation in oceanic water chemistry at appropriate scales so that this information can help the interpretation of otolith chemistry data. Otolith chemistry analysis is one of a suite of techniques that can be used to study stock structure in marine fishes. Integrating the information gained from otolith chemistry analysis with complementary techniques, such as genetics, tagging and morphometrics (e.g. Abaunza *et al.* 2008; Taillebois *et al.* 2017), will provide a powerful means to define appropriate management units for the sustainable exploitation and conservation objectives of yellowfin tuna in the Indian Ocean.

## Conflicts of interest

The authors declare that they have no conflicts of interest.

## Declaration of funding

This work was supported by a grant from the Department of Agriculture, Fishing and Alimentation from the Basque Government to Iraide Artetxe-Arrate for her doctoral studies.

## Acknowledgements

The authors acknowledge X. Salaberria for his work processing samples and J. Murua, G. Ocio and A. Sánchez for their assistance with sample collection. The authors also thank B. Orue for her guidance with environmental data analyses. This paper is contribution number 924 from AZTI Tecnalia (Marine Research Division).

## References

Abaunza, P., Murta, A. G., Campbell, N., Cimmaruta, R., Comesaña, A. S., Dahle, G., García Santamaría, M. T., Gordo, L. S., Iversen, S. A., MacKenzie, K., Magoulas, A., Mattiucci, S., Molloy, J., Nascetti, G., Pinto, A. L., Quinta, R., Ramos, P., Sanjuan, A., Santos, A. T., Stransky, C., and Zimmermann, C. (2008). Stock identity of horse mackerel (*Trachurus trachurus*) in the northeast Atlantic and Mediterranean Sea: integrating the results from different stock identification approaches. *Fisheries Research* **89**, 196–209. doi:10.1016/J.FISHRES.2007.09.022

Arai, T., Kotake, A., and Kayama, S. (2005). Movements and life history patterns of the skipjack tuna *Katsuwonus pelamis* in the western Pacific, as revealed by otolith Sr : Ca ratios. *Journal of the Marine Biological Association of the United Kingdom* **85**, 1211–1216. doi:10.1017/S0025315405012336

Bath Martin, G., and Thorrold, S. R. (2005). Temperature and salinity effects on magnesium, manganese, and barium incorporation in otoliths of larval and early juvenile spot *Leiostomus xanthurus*. *Marine Ecology Progress Series* **293**, 223–232. doi:10.3354/MEPS293223

Begg, G., Friedland, K., and Pearce, J. (1999). Stock identification and its role in stock assessment and fisheries management: an overview. *Fisheries Research* **43**, 1–8. doi:10.1016/S0165-7836(99)00062-4

Bouchoucha, M., Pécheyran, C., Gonzalez, J., Lenfant, P., and Darnaude, A. M. (2018). Otolith fingerprints as natural tags to identify juvenile fish life in ports. *Estuarine, Coastal and Shelf Science* **212**, 210–218. doi:10.1016/J.ECSS.2018.07.008

Breiman, L. (2001). Random forests. *Machine Learning* **45**, 5–32. doi:10.1023/A:1010933404324

Campana, S., and Neilson, J. (1985). Microstructure of fish otoliths. *Canadian Journal of Fisheries and Aquatic Sciences* **42**, 1014–1032. doi:10.1139/F85-127

Campbell, J. L., Babaluk, J. A., Cooper, M., Grime, G. W., Halden, N. M., Nejedly, Z., Rajta, I., and Reist, J. D. (2002). Strontium distribution in young-of-the-year Dolly Varden otoliths: potential for stock discrimination. *Nuclear Instruments & Methods in Physics Research – B. Beam Interactions with Materials and Atoms* **189**, 185–189. doi:10.1016/S0168-583X(01)01039-4

Clarke, L. M., Thorrold, S. R., and Conover, D. O. (2011). Population differences in otolith chemistry have a genetic basis in *Menidia menidia*. *Canadian Journal of Fisheries and Aquatic Sciences* **68**, 105–114. doi:10.1139/F10-147

Craig, C. A., Jarvis, K. E., and Clarke, L. J. (2000). An assessment of calibration strategies for the quantitative and semi-quantitative analysis of calcium carbonate matrices by laser ablation–inductively coupled plasma–mass spectrometry (LA-ICP-MS). *Journal of Analytical Atomic Spectrometry* **15**, 1001–1008. doi:10.1039/B002097O

Cutler, D. R., Edwards, T. C., Beard, K. H., Cutler, A., Hess, T. K., Gibson, J., and Lawler, J. J. (2007). Random forests for classification in ecology. *Ecology* **88**, 2783–2792. doi:10.1890/07-0539.1

Dammannagoda, S., Hurwood, D., and Mather, P. (2008). Evidence for fine geographical scale heterogeneity in gene frequencies in yellowfin tuna (*Thunnus albacares*) from the north Indian Ocean around Sri Lanka. *Fisheries Research* **90**, 147–157. doi:10.1016/J.FISHRES.2007.10.006

Daszykowski, M., Kaczmarek, K., Vander Heyden, Y., and Walczak, B. (2007). Robust statistics in data analysis – a review: basic concepts. *Chemometrics and Intelligent Laboratory Systems* **85**, 203–219. doi:10.1016/J.CHEMOLAB.2006.06.016

Di Franco, A., Bulleri, F., Pennetta, A., De Benedetto, G., Clarke, K. R., and Guidetti, P. (2014). Within-otolith variability in chemical fingerprints: implications for sampling designs and possible environmental interpretation. *PLoS One* **9**, e101701. doi:10.1371/JOURNAL.PONE.0101701

Elsdon, T., and Gillanders, B. (2004). Fish otolith chemistry influenced by exposure to multiple environmental variables. *Journal of Experimental Marine Biology and Ecology* **313**, 269–284. doi:10.1016/J.JEMBE.2004.08.010

Elsdon, T., and Gillanders, B. (2005). Alternative life-history patterns of estuarine fish: barium in otoliths elucidates freshwater residency. *Canadian Journal of Fisheries and Aquatic Sciences* **62**, 1143–1152. doi:10.1139/F05-029

Elsdon, T. S., Wells, B. K., Campana, S. E., Gillanders, B. M., Jones, C. M., Limburg, K. E., and Walther, B. D. (2008). Otolith chemistry to describe

movements and life-history parameters of fishes: hypotheses, assumptions, limitations and inferences. *Oceanography and Marine Biology – an Annual Review* **46**, 297–330. doi:10.1201/9781420065756.CH7

Erceg-Hurn, D., and Mirosevich, V. M. (2008). Modern robust statistical methods: an easy way to maximize the accuracy and power of your research. *The American Psychologist* **63**, 591–601. doi:10.1037/0003-066X.63.7.591

Fielding, A. H., and Bell, J. F. (1997). A review of methods for the assessment of prediction errors in conservation presence/absence models. *Environmental Conservation* **24**, 38–49. doi:10.1017/S0376892997000088

Fonteneau, A., and Hallier, J. P. (2015). Fifty years of dart tag recoveries for tropical tuna: a global comparison of results for the western Pacific, eastern Pacific, Atlantic, and Indian Oceans. *Fisheries Research* **163**, 7–22. doi:10.1016/J.FISHRES.2014.03.022

Food and Agriculture Organization of the United Nations (2016). 'The State of World Fisheries and Aquaculture 2016. Contributing to Food Security and Nutrition for All.' (FAO: Rome, Italy.)

Fowler, A., Hamer, P., and Kemp, J. (2017). Age-related otolith chemistry profiles help resolve demographics and meta-population structure of a widely dispersed, coastal fishery species. *Fisheries Research* **189**, 77–94. doi:10.1016/J.FISHRES.2017.01.010

Fraile, I., Arrizabalaga, H., Santiago, J., Goñi, N., Arregi, I., Madinabeitia, S., Wells, R. J. D., and Rooker, J. R. (2016). Otolith chemistry as an indicator of movements of albacore (*Thunnus alalunga*) in the North Atlantic Ocean. *Marine and Freshwater Research* **67**, 1002–1013. doi:10.1071/MF15097

Froese, R., and Pauly, D. (1999). *Thunnus albacares* (Bonnaterre, 1788): Yellowfin tuna. Available at https://www.fishbase.de/summary/Thunnus-albacares.html [Verified 22 October 2019].

Galland, G., Rogers, A., and Nickson, A. (2016). Netting billions: a global valuation of tuna. The Pew Charitable Trust, Washington, DC, USA.

Gibb, F., Régnier, T., Donald, K., and Wright, P. (2017). Connectivity in the early life history of sandeel inferred from otolith microchemistry. *Journal of Sea Research* **119**, 8–16. doi:10.1016/J.SEARES.2016.10.003

Hallier, J., and Fonteneau, A. (2015). Tuna aggregation and movement from tagging data: a tuna 'hub' in the Indian Ocean. *Fisheries Research* **163**, 34–43. doi:10.1016/J.FISHRES.2014.06.003

Hallier, J., and Million, J. (2012). The Indian Ocean tuna tagging programme. In 'Indian Ocean Tuna Tagging Symposium', 30 October–2 November 2012, Mauritius. pp. 1–36. (Indian Ocean Tuna Commission.) Available at https://www.iotc.org/node/4332 [Verified 22 October 2019].

Hamer, P., and Jenkins, G. P. (2007). Comparison of spatial variation in otolith chemistry of two fish species and relationships with water chemistry and otolith growth. *Journal of Fish Biology* **71**, 1035–1055. doi:10.1111/J.1095-8649.2007.01570.X

Hamer, P. A., Jenkins, G. P., and Gillanders, B. M. (2005). Chemical tags in otoliths indicate the importance of local and distant settlement areas to populations of a temperate sparid, *Pagrus auratus*. *Canadian Journal of Fisheries and Aquatic Sciences* **62**, 623–630. doi:10.1139/F04-221

Hout, M. C., Papesh, M. H., and Goldinger, S. D. (2013). Multidimensional scaling. *Wiley Interdisciplinary Reviews: Cognitive Science* **4**, 93–103. doi:10.1002/WCS.1203

Indian Ocean Tuna Commission (2017*a*). Status of the Indian Ocean yellowfin tuna (YFT: *Thunnus albacares*) resource. Available at https://www.iotc.org/sites/default/files/documents/science/species_summaries/english/Yellowfin2018.pdf [Verified 22 October 2019].

Indian Ocean Tuna Commission (2017*b*). Yellowfin tuna supporting information. Available at https://www.iotc.org/sites/default/files/documents/science/species_summaries/english/Yellowfin_tuna_Supporting_information.pdf [Verified 22 October 2019].

Indian Ocean Tuna Commission (2018). Nominal catch by species and gear, by vessel flag reporting country. IOTC-2018-DATASETS-NCDB. Available at http://www.iotc.org/documents/nominal-catch-species-and-gear-vessel-flag-reporting-country [Verified 1 November 2018].

International Seafood Sustainability Foundation (2017). Status of the world fisheries for tuna: November 2017. ISSF Technical Report 2017–02A, ISSF, Washington, DC, USA.

Izzo, C., Doubleday, Z., and Gillanders, B. (2016). Where do elements bind within the otoliths of fish? *Marine and Freshwater Research* **67**, 1072–1076. doi:10.1071/MF15064

Izzo, C., Reis-Santos, P., and Gillanders, B. M. (2018). Otolith chemistry does not just reflect environmental conditions: a meta-analytic evaluation. *Fish and Fisheries* **19**, 441–454. doi:10.1111/FAF.12264

Jones, C. M., Palmer, M., and Schaffler, J. J. (2017). Beyond Zar: the use and abuse of classification statistics for otolith chemistry. *Journal of Fish Biology* **90**, 492–504. doi:10.1111/JFB.13051

Kaji, T., Tanaka, M., Oka, M., Takeuchi, H., Ohsumi, S., Teruya, K., and Hirokawa, J. (1999). Growth and morphological development of laboratory-reared yellowfin tuna *Thunnus albacares* larvae and early juveniles, with special emphasis on the digestive system. *Fisheries Science* **65**, 700–707. doi:10.2331/FISHSCI.65.700

Kerr, L., and Campana, S. (2014). Chemical composition of fish hard parts as a natural marker of fish stocks. In 'Stock Identification Methods: Applications in Fishery Science', 2nd edn. (Eds S. Cadrin, L. Kerr, and S. Mariani.) pp. 205–234. (Academic Press: Waltham, MA, USA.)

Kerr, L., Hintzen, N., and Cadrin, S. (2017). Lessons learned from practical approaches to reconcile mismatches between biological population structure and stock units of marine fish. *ICES Journal of Marine Science* **74**, 1708–1722. doi:10.1093/ICESJMS/FSW188

Kingsford, M. J., Hughes, J. M., and Patterson, H. M. (2009). Otolith chemistry of the non-dispersing reef fish *Acanthochromis polyacanthus*: cross-shelf patterns from the central Great Barrier Reef. *Marine Ecology Progress Series* **377**, 279–288. doi:10.3354/MEPS07794

Kitchens, L., Rooker, J., Reynal, L., Falterman, B., Saillant, E., and Murua, H. (2018). Discriminating among yellowfin tuna *Thunnus albacares* nursery areas in the Atlantic Ocean using otolith chemistry. *Marine Ecology Progress Series* **603**, 201–213. doi:10.3354/MEPS12676

Kunal, S., Kumar, G., Menezes, M., and Meena, R. (2013). Mitochondrial DNA analysis reveals three stocks of yellowfin tuna *Thunnus albacares* (Bonnaterre, 1788) in Indian waters. *Conservation Genetics* **14**, 205–213. doi:10.1007/S10592-013-0445-3

Lamont, T., Barlow, R., Morris, T., and van den Berg, M. (2014). Characterisation of mesoscale features and phytoplankton variability in the Mozambique Channel. *Deep-sea Research – II. Topical Studies in Oceanography* **100**, 94–105. doi:10.1016/J.DSR2.2013.10.019

LeGrande, A. N., and Schmidt, G. A. (2006). Global gridded data set of the oxygen isotopic composition in seawater. *Geophysical Research Letters* **33**, L12604. doi:10.1029/2006GL026011

Liaw, A., and Wiener, M. (2002). Classification and regression by randomForest. *R News* **2**, 18–22.

Limburg, K. E., and Casini, M. (2018). Effect of marine hypoxia on Baltic sea cod *Gadus morhua*: evidence from otolith chemical proxies. *Frontiers in Marine Science* **5**, 482. doi:10.3389/FMARS.2018.00482

Limburg, K., Olson, C., Walther, Y., Dale, D., Slomp, C. P., and Høie, H. (2011). Tracking Baltic hypoxia and cod migration over millennia with natural tags. *Proceedings of the National Academy of Sciences of the United States of America* **108**, E177–E182. doi:10.1073/PNAS.1100684108

Limburg, K. E., Walther, B. D., Lu, Z., Jackman, G., Mohan, J., Walther, Y., Nissling, A., Weber, P. K., and Schmitt, A. K. (2015). In search of the dead zone: use of otoliths for tracking fish exposure to hypoxia. *Journal of Marine Systems* **141**, 167–178. doi:10.1016/J.JMARSYS.2014.02.014

Limburg, K. E., Wuenschel, M. J., Hüssy, K., Heimbrand, Y., and Samson, M. (2018). Making the otolith magnesium chemical calendar-clock tick: plausible mechanism and empirical evidence. *Reviews in Fisheries*

*Science & Aquaculture* **26**, 479–493. doi:10.1080/23308249.2018.1458817

Loewen, T., Carriere, B., Reist, J., Halden, N., and Anderson, W. (2016). Linking physiology and biomineralization processes to ecological inferences on the life history of fishes. *Comparative Biochemistry and Physiology – A. Molecular & Integrative Physiology* **202**, 123–140. doi:10.1016/J.CBPA.2016.06.017

Longhurst, A. R. (2007). The Indian Ocean. In 'Ecological Geography of the Sea', 2nd edn. pp. 275–320. (Academic Press: San Diego, CA, USA)

Ludsin, S., Fryer, B., and Gagnon, J. (2006). Comparison of solution-based versus laser ablation inductively coupled plasma mass spectrometry for analysis of larval fish otolith microelemental composition. *Transactions of the American Fisheries Society* **135**, 218–231. doi:10.1577/T04-165.1

Macdonald, J. I., and Crook, D. (2010). Variability in Sr : Ca and Ba : Ca ratios in water and fish otoliths across an estuarine salinity gradient. *Marine Ecology Progress Series* **413**, 147–161. doi:10.3354/MEPS08703

Macdonald, J. I., Shelley, J. M., and Crook, D. A. (2008). A method for improving the estimation of natal chemical signatures in otoliths. *Transactions of the American Fisheries Society* **137**, 1674–1682. doi:10.1577/T07-249.1

Macdonald, J. I., Farley, J. H., Clear, N. P., Williams, A. J., Carter, T. I., Davies, C. R., and Nicol, S. J. (2013). Insights into mixing and movement of South Pacific albacore *Thunnus alalunga* derived from trace elements in otoliths. *Fisheries Research* **148**, 56–63. doi:10.1016/J.FISHRES.2013.08.004

McCreary, J., Yu, Z., Hood, R., Vinaychandranc, P. N., Furuea, R., Ishido, A., and Richards, K. (2013). Dynamics of the Indian-Ocean oxygen minimum zones. *Progress in Oceanography* **112–113**, 15–37. doi:10.1016/J.POCEAN.2013.03.002

Mercier, L., Darnaude, A. M., Bruguier, O., Vasconcelos, R. P., Cabral, H. N., Costa, M. J., Lara, M., Jones, D. L., and Mouillot, D. (2011). Selecting statistical models and variable combinations for optimal classification using otolith microchemistry. *Ecological Applications* **21**, 1352–1364. doi:10.1890/09-1887.1

Olden, J. D., Joy, M. K., and Death, R. (2004). An accurate comparison of methods for quantifying variable importance in artificial neural networks using simulated data. *Ecological Modelling* **178**, 389–397. doi:10.1016/J.ECOLMODEL.2004.03.013

Paton, C., Hellstrom, J., Paul, B., Woodhead, J., and Hergt, J. (2011). Iolite: freeware for the visualization and processing of mass spectrometric data. *Journal of Analytical Atomic Spectrometry* **26**, 2508–2518. doi:10.1039/C1JA10172B

Patterson, H., Kingsford, M., and McCulloch, M. (2004). The influence of oceanic and lagoonal plume waters on otolith chemistry. *Canadian Journal of Fisheries and Aquatic Sciences* **61**, 898–904. doi:10.1139/F04-036

Paul, B., Paton, C., Norris, A., Woodhead, J., Hellstrom, J., Hergt, J., and Greig, A. (2012). CellSpace: a module for creating spatially registered laser ablation images within the Iolite freeware environment. *Journal of Analytical Atomic Spectrometry* **27**, 700–706. doi:10.1039/C2JA10383D

Pecoraro, C., Babbucci, M., Franch, R., Rico, C., Papetti, C., Chassot, E., Bodin, N., Cariani, A., Bargelloni, L., and Tinti, F. (2018). The population genomics of yellowfin tuna (*Thunnus albacares*) at global geographic scale challenges current stock delineation. *Scientific Reports* **8**, 13890. doi:10.1038/S41598-018-32331-3

Pita, A., Casey, J., Hawkins, S. J., Villarreal, M. R., Gutiérrez, M. J., Cabral, H., Carocci, F., Abaunza, P., Pascual, S., and Presa, P. (2016). Conceptual and practical advances in fish stock delineation. *Fisheries Research* **173**, 185–193. doi:10.1016/J.FISHRES.2015.10.029

Quartly, G., and Srokosz, M. (2004). Eddies in the southern Mozambique Channel. *Deep-sea Research – II. Topical Studies in Oceanography* **51**, 69–83. doi:10.1016/J.DSR2.2003.03.001

Ranaldi, M., and Gagnon, M. (2008). Zinc incorporation in the otoliths of juvenile pink snapper (*Pagrus auratus*, Forster): the influence of dietary versus waterborne sources. *Journal of Experimental Marine Biology and Ecology* **360**, 56–62. doi:10.1016/J.JEMBE.2008.03.013

Reglero, P., Tittensor, D., Álvarez-Berastegui, D., Aparicio-González, A., and Worm, B. (2014). Worldwide distributions of tuna larvae: revisiting hypotheses on environmental requirements for spawning habitats. *Marine Ecology Progress Series* **501**, 207–224. doi:10.3354/MEPS10666

Régnier, T., Augley, J., Devalla, S., Robinson, C., Wrigth, P., and Neat, F. (2017). Otolith chemistry reveals seamount fidelity in a deepwater fish. *Deep-sea Research – I. Oceanographic Research Papers* **121**, 183–189. doi:10.1016/J.DSR.2017.01.010

Reiss, H., Hoarau, G., Dickey-Collas, M., and Wolff, W. J. (2009). Genetic population structure of marine fish: mismatch between biological and fisheries management units. *Fish and Fisheries* **10**, 361–395. doi:10.1111/J.1467-2979.2008.00324.X

Rooker, J. R., Zdanowicz, V., and Secor, D. (2001). Chemistry of tuna otoliths: assessment of base composition and postmortem handling effects. *Marine Biology* **139**, 35–43. doi:10.1007/S002270100568

Rooker, J. R., Secor, D. H., Zdanowicz, V. S., De Metrio, G., and Relini, L. O. (2003). Identification of Atlantic bluefin tuna (*Thunnus thynnus*) stocks from putative nurseries using otolith chemistry. *Fisheries Oceanography* **12**, 75–84. doi:10.1046/J.1365-2419.2003.00223.X

Rooker, J. R., Secor, D. H., DeMetrio, G., Kaufman, A. J., Ríos, A. B., and Tičina, V. (2008*a*). Evidence of trans-Atlantic movement and natal homing of bluefin tuna from stable isotopes in otoliths. *Marine Ecology Progress Series* **368**, 231–239. doi:10.3354/MEPS07602

Rooker, J., Secor, D., DeMetrio, G., Schloesser, R., Block, B., and Neilson, J. (2008*b*). Natal homing and connectivity in Atlantic bluefin tuna populations. *Science* **322**, 742–744. doi:10.1126/SCIENCE.1161473

Rooker, J. R., David Wells, R. J., Itano, D. G., Thorrold, S. R., and Lee, J. M. (2016). Natal origin and population connectivity of bigeye and yellowfin tuna in the Pacific Ocean. *Fisheries Oceanography* **25**, 277–291. doi:10.1111/FOG.12154

Ruttenberg, B., Hamilton, S., and Hickford, M. (2005). Elevated levels of trace elements in cores of otoliths and their potential for use as natural tags. *Marine Ecology Progress Series* **297**, 273–281. doi:10.3354/MEPS297273

Sardenne, F., Dortel, E., Le Croizier, G., and Million, J. (2015). Determining the age of tropical tunas in the Indian Ocean from otolith microstructures. *Fisheries* **163**, 44–57. doi:10.1016/J.FISHRES.2014.03.008

Schott, F., and McCreary, J. (2001). The monsoon circulation of the Indian Ocean. *Progress in Oceanography* **51**, 1–123. doi:10.1016/S0079-6611(01)00083-0

Shi, T., and Horvath, S. (2006). Unsupervised learning with random forest predictors. *Journal of Computational and Graphical Statistics* **15**, 118–138. doi:10.1198/106186006X94072

Shiao, J., Wang, S., Yokawa, K., Ichinokawa, M., Takeuchi, Y., Chen, Y., and Shen, C. (2010). Natal origin of Pacific bluefin tuna *Thunnus orientalis* inferred from otolith oxygen isotope composition. *Marine Ecology Progress Series* **420**, 207–219. doi:10.3354/MEPS08867

Shuford, R. L., Dean, J. M., Stéquert, B., and LaBonne, M. (2007). Elemental fingerprints in otoliths of juvenile yellowfin tuna from spawning grounds in the Atlantic Ocean. *Collective Volume of Scientific Papers ICCAT* **60**, 314–329.

Stepien, C. A. (1995). Population genetic divergence and geographic patterns from DNA sequences: examples from marine and freshwater fishes. *American Fisheries Society Symposium* **17**, 263–287.

Sturrock, A. M., Hunter, E., Milton, J. A., Johnson, R. C., Waring, C. P., and Trueman, C. N. (2015). Quantifying physiological influences on otolith microchemistry. *Methods in Ecology and Evolution* **6**, 806–816. doi:10.1111/2041-210X.12381

Taillebois, L., Barton, D. P., Crook, D. A., Saunders, T., Taylor, J., Hearnden, M., Saunders, R. J., Newman, S. J., Travers, M. J., Welch,

D. J., Greig, A., Dudgeon, C., Maher, S., and Ovenden, J. R. (2017). Strong population structure deduced from genetics, otolith chemistry and parasite abundances explains vulnerability to localized fishery collapse in a large Sciaenid fish, *Protonibea diacanthus*. *Evolutionary Applications* **10**, 978–993. doi:10.1111/EVA.12499

Tanner, S., Reis-Santos, P., and Cabral, H. (2016). Otolith chemistry in stock delineation: a brief overview, current challenges and future prospects. *Fisheries Research* **173**, 206–213. doi:10.1016/J.FISHRES.2015.07.019

Tew Kai, E., and Marsac, F. (2010). Influence of mesoscale eddies on spatial structuring of top predators' communities in the Mozambique Channel. *Progress in Oceanography* **86**, 214–223. doi:10.1016/J.POCEAN.2010.04.010

Thomas, O., Ganio, K., Roberts, B., and Swearer, S. (2017). Trace element–protein interactions in endolymph from the inner ear of fish: implications for environmental reconstructions using fish otolith chemistry. *Metallomics* **9**, 239–249. doi:10.1039/C6MT00189K

Thorrold, S. R., Jones, G. P., Planes, S., and Hare, J. A. (2006). Transgenerational marking of embryonic otoliths in marine fishes using barium stable isotopes. *Canadian Journal of Fisheries and Aquatic Sciences* **63**, 1193–1197. doi:10.1139/F06-048

Tibshirani, R., Walther, G., and Hastie, T. (2001). Estimating the number of clusters in a data set via the gap statistic. *Journal of the Royal Statistical Society – B. Statistical Methodology* **63**, 411–423. doi:10.1111/1467-9868.00293

Tournois, J., Darnaude, A. M., Ferraton, F., Aliaume, C., Mercier, L., and McKenzie, D. J. (2017). Lagoon nurseries make a major contribution to adult populations of a highly prized coastal fish. *Limnology and Oceanography* **62**, 1219–1233. doi:10.1002/LNO.10496

van Hulten, M., Middag, R., Dutay, J., De Baar, H., Roy-Barman, M., Gehlen, M., Tagliabue, A., and Sterl, A. (2017). Manganese in the West Atlantic Ocean in context of the first global ocean circulation model of manganese. *Biogeosiences* **14**, 1123–1152. doi:10.5194/BG-14-1123-2017

Venables, W. N., and Ripley, B. D. (2002). 'Modern Applied Statistics with S', 4th edn. (Springer: New York, NY, USA.)

Volk, E. C., Blakley, A., Schroder, S. L., and Kuehner, S. (2000). Otolith chemistry reflects migratory characteristics of Pacific salmonids: using otolith core chemistry to distinguish maternal associations with sea and freshwaters. *Fisheries Research* **46**, 251–266. doi:10.1016/S0165-7836(00)00150-8

Walther, B. D., and Thorrold, S. (2006). Water, not food, contributes the majority of strontium and barium deposited in the otoliths of a marine fish. *Marine Ecology Progress Series* **311**, 125–130. doi:10.3354/MEPS311125

Wang, C. H., Lin, Y. T., Shiao, J. C., You, C. F., and Tzeng, W. N. (2009). Spatio-temporal variation in the elemental compositions of otoliths of southern bluefin tuna *Thunnus maccoyii* in the Indian Ocean and its ecological implication. *Journal of Fish Biology* **75**, 1173–1193. doi:10.1111/J.1095-8649.2009.02336.X

Webb, S. D., Woodcock, S. H., and Gillanders, B. M. (2012). Sources of otolith barium and strontium in estuarine fish and the influence of salinity and temperature. *Marine Ecology Progress Series* **453**, 189–199. doi:10.3354/MEPS09653

Wells, R. D., Rooker, J. R., and Itano, D. G. (2012). Nursery origin of yellowfin tuna in the Hawaiian Islands. *Marine Ecology Progress Series* **461**, 187–196. doi:10.3354/MEPS09833

Wells, R. J. D., Kinney, M., Kohin, S., Dewar, H., Rooker, J. R., and Snodgrass, O. (2015). Natural tracers reveal population structure of albacore (*Thunnus alalunga*) in the eastern North Pacific. *ICES Journal of Marine Science* **72**, 2118–2127. doi:10.1093/ICESJMS/FSV051

Wiggert, J., Murtugudde, R., and Christian, J. (2006). Annual ecosystem variability in the tropical Indian Ocean: results of a coupled bio-physical ocean general circulation model. *Deep-sea Research – II. Topical Studies in Oceanography* **53**, 644–676. doi:10.1016/J.DSR2.2006.01.027

Wilcox, R. (2012). 'Introduction to Robust Estimation and Hypothesis Testing', 3rd edn. (Academic Press: Waltham, MA, USA.)

Wolf, R., and Wilson, S. (2007). USGS reference materials program. Serving the needs of the global analytical community. USGS Fact Sheet 2007–3056, US Geological Survey, Denver, CO, USA.

Woodcock, S., Munro, A., Crook, D., and Gillanders, B. (2012). Incorporation of magnesium into fish otoliths: determining contribution from water and diet. *Geochimica et Cosmochimica Acta* **94**, 12–21. doi:10.1016/J.GCA.2012.07.003

Wright, P. J., Régnier, T., Gibb, F. M., Augley, J., and Devalla, S. (2018). Assessing the role of ontogenetic movement in maintaining population structure in fish using otolith microchemistry. *Ecology and Evolution* **8**, 7907–7920. doi:10.1002/ECE3.4186

Zeileis, A., and Grothendieck, G. (2005). zoo: S3 infrastructure for regular and irregular time series. *Journal of Statistical Software* **14**, 1–27. doi:10.18637/JSS.V014.I06

Zhang, C., Ye, Z., Li, Z., Wan, R., Ren, Y., and Dou, S. (2016). Population structure of Japanese Spanish mackerel *Scomberomorus niphonius* in the Bohai Sea, the Yellow Sea and the East China Sea: evidence from random forests based on otolith features. *Fisheries Science* **82**, 251–256. doi:10.1007/S12562-016-0968-X

Zudaire, I., Murua, H., Grande, M., and Bodin, N. (2013). Reproductive potential of yellowfin tuna (*Thunnus albacares*) in the western Indian Ocean. *Fishery Bulletin* **111**, 252–264. doi:10.7755/FB.111.3.4

Handling Editor: Bronwyn Gillanders